

A Case Study in Aerodynamic Design and Analysis of the Rear Wing of a High Performance Vehicle

Bruno R. M. Padilha
Guilherme N. Barufaldi
Roberto G. A. da Silva

Instituto Tecnológico de Aeronáutica

ABSTRACT

One of the most important trade-offs of the aerodynamic design of a competition vehicle is the balance between drag and downforce. On the one hand, the vehicle must be able to achieve high speeds, especially on straight lines, and this means that the drag force must be kept as low as possible. On the other hand, in order to reach high turning performance, the aerodynamic devices must produce high levels of downforce, and the price paid is a substantial increase in drag force. To obtain the best possible aerodynamic design – and the best possible trade-off between drag and downforce – engineers usually resort to knowledge and tools from the aeronautical industry. In this paper, we present a case study about the development of the rear wing of a high performance vehicle currently being designed for the Brazilian Endurance Championship (P1 category). The design process is divided into two parts: the 2-D analysis, in which the wing profile is selected; and the 3-D analysis, in which the wing shape is conceived. In both phases, analytical and computational tools were employed, including computational fluid dynamics (CFD) software. The paper also describes the utilization of a Gurney flap, considerations about airfoils, Reynolds number, and how the relation between drag and downforce is evaluated.

INTRODUCTION

Historically, the adaptation of wings to competition cars was initiated in May 1962 by Henry “Smokey” Yunick, for the Indianapolis 500 Mile Race. This is considered the starting point for understanding aerodynamics as a determining factor in the success of a high performance vehicle design. The innovative car presented by Yunick ended up being banned from the race that year, but the results of the idea grew popular throughout the 1960s, in several categories of world motorsport.

Since its introduction in the 1960s, the evolution of race car aerodynamics has been remarkable. When in high speeds, high-performance vehicles are currently capable of

generating thousands of kilograms of downforce [1], both in open-wheel categories, such as Formula 1 and Indy, and in high-performance endurance prototype categories, such as the WEC (*World Endurance Championship*) and the IMSA (*International Motor Sports Association*).

Such impressive numbers are achievable thanks not only to the development of wings, but also of the bodywork as a whole. This evolution was only possible through a combination of experimental methods in wind tunnels, and numerical tools, such as computational fluid dynamics (CFD) and panel methods. However, due to their practicality and relatively lower costs, numerical tools have become the standard means for aerodynamic analysis during the conceptual design phase.

Although the bodywork can produce a significant amount of the total downforce, not all vehicles are able to take advantage of its shape to produce lift. Therefore, the most common lift-producing device used in race cars is the wing. Its design process is usually divided into two phases: the development of the profile – i.e., the two-dimensional shape of the wing cross section – and the development of the three-dimensional wing shape [2].

The wing profile design is highly dependent on the Reynolds number expected for the design point, and also on the wing downforce requirements. If the wing dimensions are constrained by regulations or design requirements, and if the angle of attack cannot be variable, which is the most common situation for race cars, then the airfoil must be able to produce a large pressure difference between its upper and lower surfaces. This can be achieved by using high-lift devices, such as trailing edge flaps.

For a competition race vehicle, the three-dimensional shape of the wing is usually determined or constrained by regulations. Regardless, the two main design variables to consider are span and chord length, i.e., the longitudinal distance between the leading and trailing edges. If the wing span is limited to the vehicle width, or another reference

length, then the chord distribution will determine the wing planform shape. When integrated to the bodywork, the wing incidence relative to a reference line will determine the reference angle of attack. If the competition regulation allows it, the incidence can be adjusted for a particular race track.

This work presents the development of a rear wing for a new car prototype that is currently being designed for the Brazilian Endurance Championship, in the P1 Category. The competition regulation does not impose aerodynamic constraints on the design. However, the vehicle is being conceived to be marketed in other similar competitions in Latin America, so the development team has adopted international regulations. Therefore, the aerodynamic design follows guidelines imposed by the “Le Mans Prototype Class 3” (LMP3), issued by the “Automobile Club de l’Ouest” (ACO), the organising entity behind the annual Le Mans 24 Hours race. The LMP3 regulation [3] is also applied in the European Le Mans Series, and the Asian Pacific Le Mans Series.

The aim of this project is to develop a rear wing that is compliant with the LMP3 Regulations design requirements, and able to meet specific performance goals established by the design team. Since the prototype car is still under development, specific performance standards and goals are kept undisclosed. However, the criteria used for performance analysis were formulated according to historical data presented in [4]. This article presents the development of both the wing profile and planform. Relevant aerodynamic characteristics are shown, together with the methodologies applied.

WING PROFILE DESIGN

The LMP3 Regulations in [3] impose geometric constraints for lift-generating devices. A maximum of two elements are allowed in the wing: the main wing element and a trailing edge flap. The main element chord shall not be greater than 300 mm, and the flap chord shall not be greater than 1/3 of the main element chord. An additional gurney flap is allowed, but its height is restricted to 30 mm. Since the wing planform dimensions are constrained by regulations, and a variable incidence wing is not allowed, the remaining resource able to increase lift-generating capability is the wing profile. Therefore, a profile capable of producing a high lift coefficient is required [2].

The wing profile or airfoil is the two-dimensional shape defined by the intersection of the wing with an imaginary plane that is perpendicular to its transverse axis [5]. A two-element profile was developed for this project (Fig. 1), by combining well-known aeronautical airfoils designed for operations in low Reynolds number conditions.



Figure 1: Two-element wing profile developed for the project.

The profile is composed of a main element and a flap, with an additional gurney flap at the rearmost trailing edge. Based on regulations constraints, the flap chord was fixed at 1/3 of the main element chord, the maximum relative length allowed. Both elements share the same baseline geometry, extracted from a highly cambered airfoil.

The main performance parameters for evaluating a wing profile (airfoil) are its lift coefficient c_l , and drag coefficient c_d , defined according to Eqs. (1) and (2), respectively [2].

$$c_l = \frac{L'}{q_\infty \bar{c}} \quad (1)$$

$$c_d = \frac{D'}{q_\infty \bar{c}} \quad (2)$$

where L' is the lift force per span unit; D' is the drag force per span unit q_∞ is a reference dynamic pressure, and \bar{c} is the profile chord. Both coefficients are dimensionless and can be calculated from experimental data, or directly obtained from software. The most commonly used parameter for measuring the airfoil efficiency is its lift-to-drag ratio c_l/c_d .

Another significant design variable is the position of the flap with respect to the main element. According to [6], flaps with incidence angles greater than 30° with respect to the main element reference line show inferior c_l/c_d values, even if a higher value of c_l is achieved. This implies that, for a given value of c_l , a higher drag is created, hence a lower efficiency is achieved. Since this wing is intended for an endurance vehicle, excessive drag values will significantly reduce its autonomy, resulting in more pit-stops.

Regarding the flap position, two other factors are essential for adequate element integration: the overlap, i.e., the distance between the flap leading edge and the main element trailing edge; and the gap, i.e., the distance between the flap upper surface and the main element lower surface. The flap incidence, overlap and gap were defined according to criteria presented in [6] for improving c_l/c_d ratio: a 30° flap incidence; a 5.2% overlap; and a 3.8% gap (values in percentage of the complete profile chord). The gurney flap is perpendicular to the flap chord, and its height is 2% of the complete profile chord.

The gurney flap at the trailing edge creates a boundary layer separation [7] that makes it difficult to calculate airfoil coefficients using regular panel method codes. Therefore, a CFD analysis was employed. Figures 2 and 3 show CFD results for the profile lift coefficient (c_l) and drag coefficient (c_d), respectively.

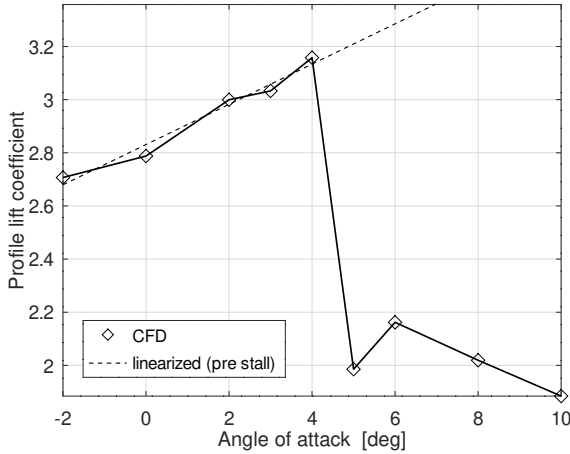


Figure 2: Profile lift coefficient versus angle of attack. Points from CFD analysis and pre stall linearized model – $Re = 6 \times 10^6$.

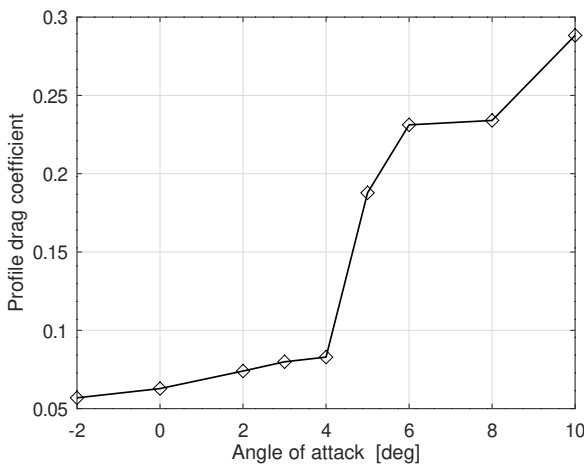


Figure 3: Profile drag coefficient versus angle of attack. Points from CFD analysis – $Re = 6 \times 10^6$.

Since atmospheric conditions vary during a race, as well as vehicle speed, the Reynolds number (Re) of the airflow over the wing does not remain constant. According to [1], the average Reynolds number for the airflow over a high-performance vehicle wing is 6×10^6 – this value of Re was employed for the 2-D CFD analyses.

Figure 2 shows that the airfoil developed for this project is capable of achieving high c_l values when compared to existing profiles [5]. The airfoil stall begins at an angle of attack of approximately 4° . A linearized model for the c_l vs. α points (pre stall) is presented, as it is required for the methodology employed in the finite wing design.

FINITE WING DESIGN

The wing planform is defined mostly by the regulations constraints on dimensions [3]. With chord length and wingspan defined, a linear lifting line algorithm is employed for the initial aerodynamic analysis of the finite, three-dimensional wing without wingtip devices. The linear lifting line theory is the most traditional three-dimensional wing model [2], and provides many useful informations. Due to its low computational cost, this model is employed to guide the more complex and computationally demanding CFD analyses.

For a rectangular wing, the spanwise lift distribution is symmetrical, with the highest values of circulation and local lift (c_l) happening at the wing center line [2]. The algorithm is applied to a pre-defined range of angle of attack (α) values, and the maximum local lift is observed for each α . The wing stall is estimated with the critical section criterion: when the maximum local lift equals the maximum profile lift coefficient (from the chart in Fig. 2), the wing is defined to be at the stall condition. The wing lift coefficient (C_L) at this point is defined as the maximum lift coefficient, and the angle of attack is defined as the angle of stall.

Figure 4 shows the maximum local lift obtained within the wing (at the center line) as a function of the angle of attack. The maximum local lift equals the maximum profile lift coefficient when the wing angle of attack is approximately 11° .

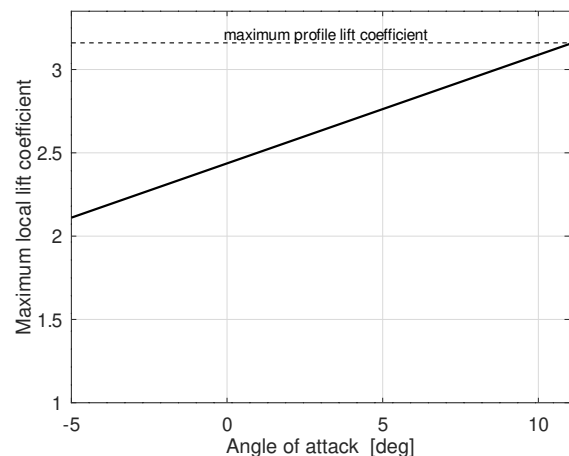


Figure 4: Maximum local lift coefficient within the wingspan versus wing angle of attack.

Figure 5 shows the lift distribution along the semi wingspan when the wing reaches the stall condition ($\alpha \approx 11^\circ$). Since the distribution is symmetrical, only half of the wing is shown. One should notice that the maximum c_l is reached at the center line.

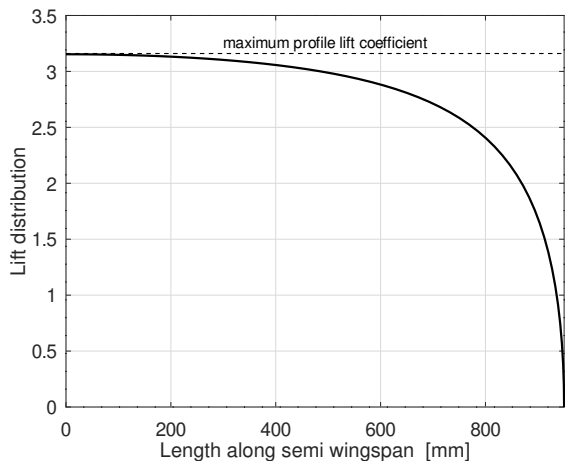


Figure 5: Lift distribution (local c_l) along the semi wingspan when the wing is at its maximum lift coefficient.

Once the angle of stall and the maximum lift coefficient are determined, the lifting line analysis is concluded. The finite wing lift coefficient C_L , and total drag coefficient C_D are defined according to Eqs. (3) and (4), respectively.

$$C_L = L/q_\infty S \tag{3}$$

$$C_D = D/q_\infty S \tag{4}$$

where L is the wing lift; D is the wing total drag; and S is the wing reference area. Figure 6 shows the wing lift coefficient C_L as a function of the angle of attack.

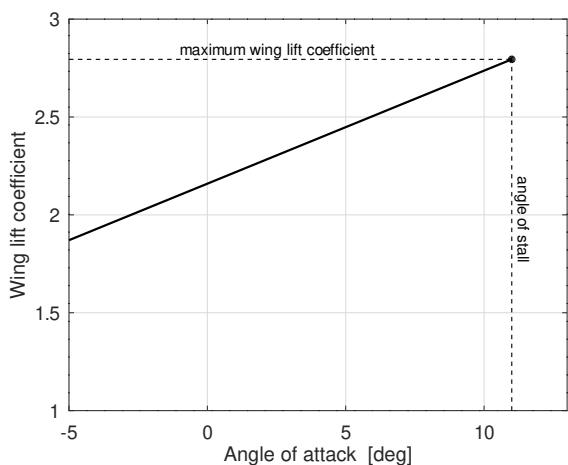


Figure 6: Wing lift coefficient (C_L) versus angle of attack.

Figure 7 shows the wing total drag coefficient (C_D) as a function of the lift coefficient. This curve is known as drag polar, and Fig. 7 exhibits the segment relative to the interval considered in the analysis.

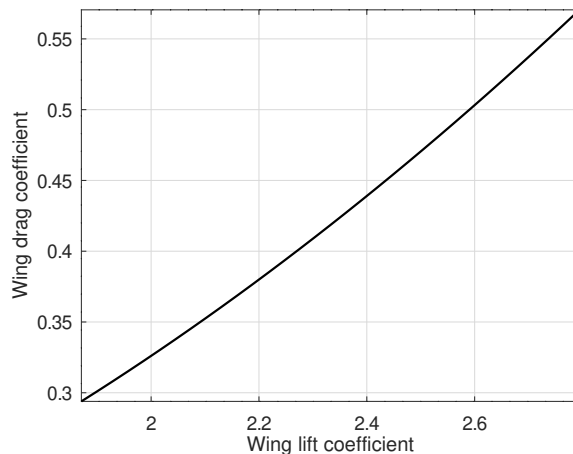


Figure 7: Wing drag polar segment: drag coefficient C_D versus lift coefficient C_L .

The drag coefficient values observed in the wing drag polar are quite high when compared to regular airplane wings [2]. These high values are due to the fact that the wing presented in this work operates with C_L values significantly higher than regular airplane wings during cruise flight. The drag portion due to lift is known as induced drag, and is proportional to the square of the lift coefficient. Figure 8 shows the induced drag as a percentage of the total wing drag versus the angle of attack. The chart in Fig. 8 provides an illustration of how significant the induced drag is in this particular wing performance.

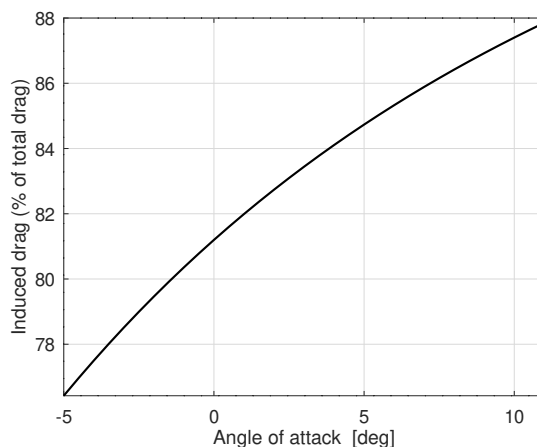


Figure 8: Induced drag as a percentage of total drag versus wing angle of attack.

An important figure to consider when evaluating a wing performance is the wing lift-to-drag ratio L/D . This ratio represents an efficiency parameter: if two equivalent wings are compared, for a given C_L value, the one with the highest L/D produces less drag. Figure 9 shows the wing lift-to-drag ratio and the lift coefficient, both as functions of the angle of attack. In the α interval considered, the higher the angle of attack, the higher the C_L value and the lower the L/D value.

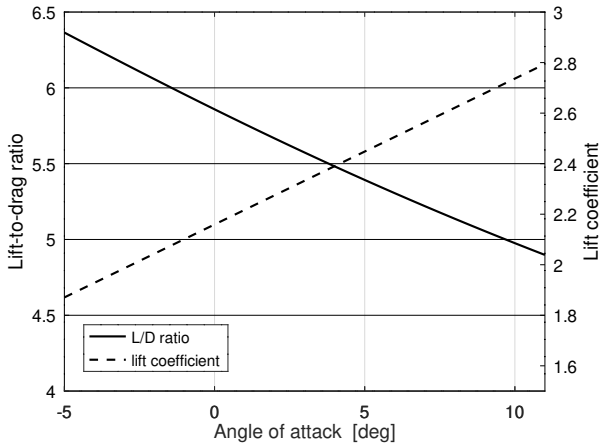


Figure 9: Wing lift-to-drag ratio and lift coefficient as functions of the angle of attack.

ENDPLATES AND CFD ANALYSIS

The chart in Fig. 8 shows that the induced drag represents a major contribution to the total drag. One way to mitigate this effect is to take advantage of the wing fixing structure and extend it to cover the wing tips. The resulting structures form plates that are orthogonal to the wing transverse axis and are called endplates. Figure 10 shows the complete wing with endplates.

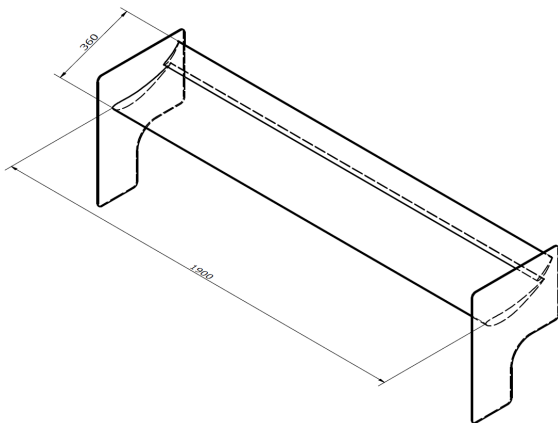


Figure 10: Perspective view of the complete wing, with endplates. Drawing dimensions are in mm.

However, the endplates cannot be modeled with the lifting line theory. To overcome this limitation and compute the complete wing coefficients, a CFD analysis is conducted. Moreover, the lifting line theory does not account for cross air flow on the wing surfaces, which may happen in the case of strong pressure gradients, i.e., of high C_L values. The main function of the linear lifting line algorithm is to provide quick computations, which are especially needed during the initial design phases, and to guide wind tunnel experiments and CFD runs.

The endplate design follows criteria presented in [6], where the author show empirical data about the pressure gradients found at the wingtip. Endplates help reduce the gradients and slow down the flow from the wing upper surface (lower pressure) to the lower surface (higher pressure). The result is an increase in lift and a decrease in drag.

The control volume adopted for the CFD simulations is shown in Fig. 11. The volume edge sizes were calculated based on wing chord c and span b .

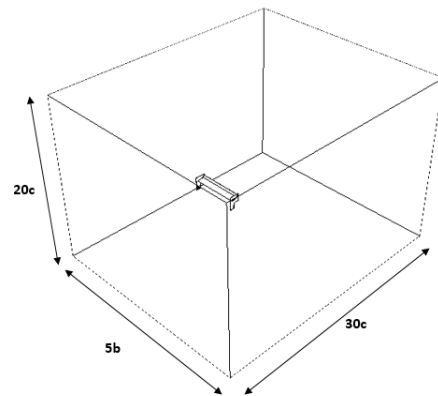


Figure 11: Control volume adopted for the CFD simulations. Drawing dimensions are given as multiples of the wing chord c and span b .

The mesh inside the control volume is unstructured, and is composed by tetrahedral elements, as shown in a sectional view in Fig. 12. To better capture aerodynamic phenomena, the mesh is locally refined as it approaches the wing. At the wing surface, the elements dimensions vary between 1 and 3 mm – for comparison, the wingspan is 1900 mm and the chord is 360 mm. The control volume features a central region with local mesh element refinements, extending to the side walls of the control volume, where the elements are limited to 50 mm. Such refinements are necessary to improve the capture of the turbulence wake and the final drag values [8]. To improve the capture of the boundary layer an inflation is inserted in the mesh, with 10 layers of prismatic elements over the wing. On average, the complete meshes featured 18 million elements.

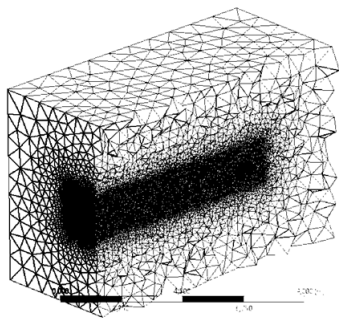


Figure 12: Sectional view of the unstructured mesh.

The simulations were performed in the Ansys Fluent™ CFD software, with the mesh described above. Flow conditions were set with the Standard Atmosphere (ISA) model, with a static pressure of 9.364×10^4 Pa, temperature of 27°C , and air density of 1.225 kg/m^3 . The turbulence model adopted is the SST k- ω . Simulation convergences were obtained between 800 to 2000 iterations, with residuals on the order of 1–4.

Figure 13 shows wing lift coefficient values obtained from CFD simulations, for two different angles of attack, and two wing configurations (with and without endplates). For reference, the lifting line (LL) prediction is also displayed. The endplates help increase lift generation for the same angle of attack, as expected. Also as expected, the LL prediction yields slightly overestimated C_L values, since it does not account for cross flows and other viscous effects.

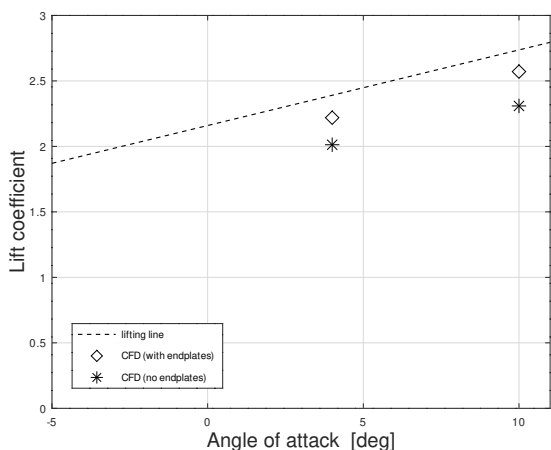


Figure 13: Comparison between wing lift coefficients (C_L) predicted by lifting line theory and CFD (with and without endplates).

Figure 14 shows total drag coefficient values obtained from CFD simulations, for the same wing configurations (with and without endplates). For reference, the drag po-

lar predicted by the lifting line algorithm is also displayed. The endplates help reduce drag generation, as expected. It is worth noting that the drag values predicted by CFD for the wing without endplates agree very well with the drag polar obtained from LL, with the differences in predictions decreasing as C_L increases. This is due to the fact that the induced drag becomes more predominant as lift increases (as shown in Fig. 8). Since the relative drag parcel due to viscous effects is reduced as C_L is increased, LL drag predictions tend to become more accurate.

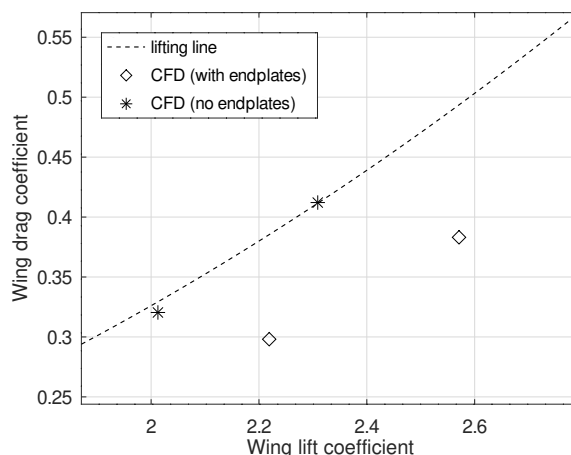


Figure 14: Comparison between drag polar points predicted by lifting line theory and CFD (with and without endplates).

Figure 15 shows lift-to-drag ratio values obtained from CFD simulations, for the same situations. For reference, the LL lift-to-drag ratio prediction is also displayed.

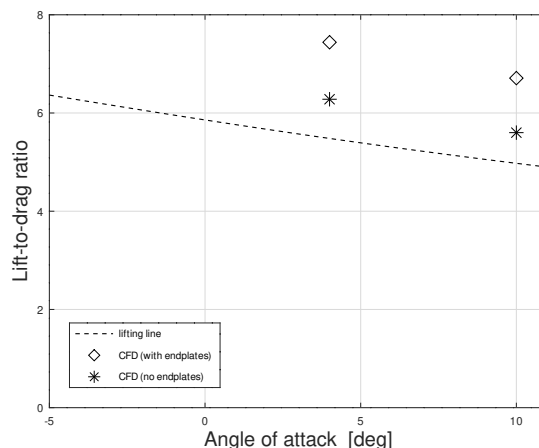


Figure 15: Comparison between lift-to-drag ratios predicted by lifting line theory and CFD (with and without endplates).

From the chart in Fig. 15, one can notice that the endplates significantly improve L/D values. This improvement

is due to the fact these devices simultaneously increase lift and decrease drag. This effect is known, and is explained in more detail in [6]. Wing aerodynamic properties agree with the values presented in [4].

The wing incidence with respect to the vehicle reference axis is usually adjusted for each racing circuit. Tracks with more corners, or with tighter corners – or equivalently, slower tracks – demand higher C_L values, because more downforce is required at relatively lower speeds. Faster tracks, especially those with longer straights, require lower C_L values, since more drag reduces top speeds.

CONCLUSION

This work has presented the aerodynamic design and analysis of the rear wing of a high-performance vehicle currently being built for the Brazilian Endurance Championship. Due to geometric constraints imposed by competition regulations, the wing must be able to develop high lift coefficient values. A multi-element wing profile was designed and presented, together with relevant aerodynamic properties obtained from CFD analysis. The three-dimensional (finite) wing design is also shown, and two distinct methodologies are applied for the aerodynamic analyses: the lifting line theory and computational fluid dynamics. The main aerodynamic wing properties were presented, and are compatible with those found in literature. Although the airfoil is capable of generating high c_l values, it also produces significant amounts of drag due to the high camber and the gurney flap. It was concluded that the wing can significantly improve the performance of the vehicle for which it was designed. For future works, opti-

mization methods can be applied to reduce profile drag and improve the wing lift-to-drag ratio.

REFERENCES

- [1] Katz, J., *Race Car Aerodynamics: Designing for Speed*, Bentley Publishers, Cambridge, MA, 2nd ed., 1996.
- [2] Anderson, Jr., J. D., *Fundamentals of Aerodynamics*, McGraw-Hill Education, New York City, NY, 5th ed., 2010.
- [3] “2020 Technical and Sporting Regulations,” European Le Mans Series, retrieved September 12, 2020.
- [4] Toet, W., “Aerodynamics and aerodynamic research in Formula 1,” *The Aeronautical Journal*, Vol. 117, No. 1187, January 2013.
- [5] Abbott, I. H. and von Doenhoff, A. E., *Theory of Wing Sections*, Dover Publications, New York City, NY, 2nd ed., 1959.
- [6] McBeath, S., *Competition Car Aerodynamics*, Veloce Publishing Limited, Dorchester, 3rd ed., 2017.
- [7] Jeffrey, D., Zhang, X., and Hurst, D. W., “Aerodynamics of Gurney Flaps on a Single-Element High-Lift Wing,” *Journal of Aircraft*, Vol. 37, No. 2, January 2000.
- [8] Anderson, Jr., J. D., *Computational Fluid Dynamics*, McGraw-Hill Education, New York City, NY, 1st ed., 1995.